17th International Conference on Probabilistic Safety Assessment and Management &
Asian Symposium on Risk Assessment and Management (PSAM17&ASRAM2024)
7-11 October, 2024, Sendai International Center, Sendai, Miyagi, Japan

Development of a risk indicator for ship drifting groundings

Spencer August Dugan[a]*, Ingrid Bouwer Utne[a]
[a] Department of Marine Technology (IMT), NTNU, Trondheim, Norway

Abstract: The maritime industry has repeatedly experienced severe accidents resulting from drifting ships. This paper develops a risk indicator for drifting groundings called "time to grounding" (TTG). The indicator incorporates the ship's location, local environmental conditions, and local water depths to provide early warnings for accident prevention. The paper describes the methodology used to calculate TTG and the data sources that are required. The methodology is applied to historical voyage data for a research ship operating on the Norwegian coast. The values of TTG are presented over the course of a voyage with diverse navigational and environmental conditions. The application and interpretation of the risk indicator is discussed for monitoring ship traffic and for the risk-based control and risk perception of autonomous ships.

Keywords: maritime safety, transportation risk, grounding, risk indicator

1. INTRODUCTION

The maritime industry has been plagued by significant accidents in which drifting ships ground. After jamming her rudder to avoid a collision, the *Amoco Cadiz*, grounded on the coast of Brittany in 1978, resulting in the largest oil spill of its kind at the time and incalculable damage to marine life [1]. In 2000, the bow section of the *Nakhodka* grounded in the Sea of Japan after the ship broke in two during severe weather. The result was the largest oil spill in Japan's history [2]. Two other serious accidents, the Northern Cape oil spill [3] and the fatal grounding of the *Selendang Ayu* [4], developed similarly: the ships initially lost propulsion and subsequently drifted ashore. To prevent similar accidents, the IMO has mandated the use of vessel traffic services (VTS) in coastal countries for the purpose of ship traffic monitoring and emergency response [5]. However, there have still been several accidents in recent years initiating from the reduction or loss of propulsion. These include the groundings of the *Nenita* in 2016 [6], the *Thea II* in 2018 [7], and the *Triesta Star* in Reunion Island in 2022 [8]; the near-miss of the *Viking Sky* in 2019 [9]; and the collision of the *Julietta D* with a wind farm and tanker in 2022 [10].

A reduction or loss in propulsion leads to limited maneuverability of the ship. The subsequent drifting behavior (i.e., the speed and direction) of ships is important to predict in order to potentially prevent maritime accidents. Accurate prediction of a ship's drifting behavior enables better emergency response preparedness [11] and allows for allocation of resources when applied to maritime traffic projections [12]. However, drift trajectory prediction is complex and the methods to do so rely on several modeling assumptions and/or suffer from limited experimental data for verification.

For these reasons, we aim to develop a risk indicator to assess a ship's "time to grounding" (TTG). Risk indicators are operational variables that can be used to describe the condition that a system is experiencing [13]. Risk indicators are quantifiable, rooted in the principles of risk analysis, and updated at regular intervals for monitoring or early warning purposes [14, 15]. For drifting groundings, the TTG incorporates the ship's location and dimensions, environmental conditions, and grounding hazards.

This paper presents the method to calculate the expected TTG. We use commonly available information and simple hydrodynamic techniques to ensure that the method is reproducible and computationally efficient. The TTG is computed and presented at sampled points of a historical coastal voyage of a research ship in Norway. The purpose of this application is to demonstrate the variability of the indicator as the ship's navigational and environmental conditions vary during the voyage.

The structure of the paper is as follows: the next section presents drifting groundings as an accident mode and surveys the literature on drift trajectory prediction. Section 3 presents the overall methodology to determine the

TTG using a prediction of drifting speed and direction and nearby depth information. Section 4 presents the results of the case study. Section 5 discusses the major findings.

2. LITERATURE REVIEW

2.1. Drifting grounding risk models

Grounding refers to the impact of a ship on the seabed or waterway side [16]. The IMO casualty code distinguishes between two types of groundings: those that occurred while the ship was under power and those that occurred while the ship was drifting [17]. The latter is referred to as drifting grounding and is the subject of this analysis.

A typical narrative for a drifting grounding begins with the ship experiencing a reduction or complete loss of available propulsion power, electrical power, or steering capability. The ship is subjected to environmental forces that cause it to drift in a certain direction while the failure is repaired. The ship may also attempt to anchor in order to arrest its drift, or requisition a tugboat. A grounding occurs when these actions do not prevent the ship from striking the seabed. High profile examples of drifting groundings can be further studied in the following accident reports: [3, 4, 7, 8].

The risk of drifting grounding has been modeled in several quantitative risk assessments [18, 19, 20]. These assessments rely on estimates of ship failure frequency and the probabilities of successful emergency towing, anchoring, and successful repairs. The role of environmental conditions is simplified in the assessments; Friis-Hansen [19] and Kystverket [20] use a uniform drift speed distribution between 1 and 3 m/s. Fowler and Sørgård [18] models the drift speed as 0.3 m/s in calm wind conditions and 0.9 m/s in stormy conditions. All equate the drift direction with the direction of the wind.

2.2. Drift force prediction models

Studies attempting to frame the drift mechanics problem begin with Newman [21], who outlined the hydrodynamic forces and showed theoretically that the stable response of the ship is perpendicular to its drifting direction (i.e., a hull drift angle of 90°). Ueno and Nimura [22] investigated the steady-state drifting behavior in waves using experiments and panel methods. Yasukawa et al. [23] conducted experiments using a bulk carrier model to investigate the drifting behavior of dead ships in wind. The findings include approximate drift angles for both the full load and ballast condition, and validation of a simulation method to model this behavior. A simulation model incorporating the effects of wind and waves was developed by Yasukawa et al. [24], and validated using experimental data from bulk carrier model tests.

Sørgård and Vada [25] developed a drift trajectory prediction tool using two primary components: 1) estimating ocean current velocities, and 2) predicting the forced drift on a ship caused by wind and wave forces. Furthermore, the authors compare their model predictions to 26 observations of large tankers drifting for one hour in the North Sea. The model by Sørgård and Vada [25] is also used in the ShipDrift module from the OpenDrift package [26].

3. METHODOLOGY

This section presents the methodology to calculate the TTG using the ship's position, the environmental conditions, and the surrounding water depths. For each time stamp, the following step-wise procedure occurs:

1. Retrieve vessel coordinates (longitude and latitude) from voyage data.
2. Input vessel coordinates and timestamp to historical ocean forecast models to obtain wind speed, wind direction, wave height, wave period, wave direction, and sea-water velocity and direction.
3. Predict environmental forces using ship characteristics to estimate the drifting speed and direction of the ship. Iterate until a stable solution is found. Sum the forced drift speed vector and sea-water velocity vector for the resultant drift speed and direction.

4. Model the drifting direction as a normal distribution. Determine the nearest grounding points for a sampled number of angles.
5. Divide the distance to ground by the expected drift speed at each angle. Perform a probabilistic weighted sum to determine the overall TTG.

Subsections 3.1, 3.2, and 3.3 present more information on the forced drift speed and direction prediction method, the calculation of the time to grounding, and the data sources, respectively.

3.1. Drift speed and direction

To predict the drift speed and direction, we closely follow the methodology developed by Sørgård and Vada [25] because of its computational simplicity and validation using experimental observations. This subsection presents the main equations of interest. When the equation is used from [25], it is preceded by a citation indication. All deviations from the methodology in are described below.

The overall drift speed is comprised of two components: the sea-water velocity (a function of tidal and ocean currents) and the forced drift velocity, a function of the acting environmental forces on the ship. The resultant speed and direction in vector form is obtained as follows [25]:

$$\boldsymbol{v_d} = \boldsymbol{v_o} + \boldsymbol{v_w} \tag{1}$$

where $\boldsymbol{v_o}$ is the sea-water velocity and $\boldsymbol{v_w}$ is the forced drift velocity caused by wind and wave forces on the ship. Sea-water velocities are obtained from historical forecast data from the NorKyst model (see Section 3.3). The forced drift velocity is predicted below.

The acting forces on the ship of interest are the wind drag force, the mean wave drift force, the wave damping force, and the ship form drag. The resultant force, $\boldsymbol{F}$, will act in the direction θ. The experimental results from Sørgård and Vada [25] show that the wind damping is minimal compared to the wind and wave drag forces, and can be neglected. Furthermore, the equilibrium or steady-state drift behavior is reached within 5-10 minutes, allowing us to disregard the consideration of the vessel's initial forward speed.

The wind force is applied in the direction of the wind, α [25]:

$$F_{wind} = \frac{1}{2}\rho_a C_F A_{cwp} V_{wind}^2 \tag{2}$$

where ρ_a is the density of air, C_F is the drag coefficient and a function of deck height (refer to [25] for more details), A_{cwp} is the cross wind profile area of the ship, and V_{wind} is the averaged wind speed at 10-m above sea level.

The wave drift force, F_{wave}, and damping, D, are dependent on the ship's seakeeping characteristics and the encountered wave energy spectrum. The wave drift force is applied in the direction of the waves, ϕ. The wave damping is applied to the opposite direction of the ship drift, and is proportional to the resultant drift speed of the ship [25]:

$$F_{wave} = \sum_{j=1}^{N} S^2(j\Delta\omega)G(j\Delta\omega) \tag{3}$$

$$D = \sum_{j=1}^{N} S^2(j\Delta\omega)H(j\Delta\omega) \tag{4}$$

where $H(\omega)$ and $G(\omega)$ are transfer functions for the mean wave drift force and wave damping, and $S(\omega)$ represents the sea spectrum. In all cases, ω represents the angular frequency of the waves. The wave force and damping

transfer functions were reproduced from Sørgård and Vada [25] and interpolated for ratios of ship beam to length (B/L) and ship draft to length (T/L).

We depart from the methodology of [25] by using the JONSWAP sea spectrum rather than the Pierson-Moskowitz spectrum. The JONSWAP spectrum has a higher peak, and has been demonstrated to have stronger agreement with wave spectrums in coastal areas [27]. The wave energy spectrum for the JONSWAP spectrum is parameterized using the significant wave height and mean wave period (refer to [28] for more information).

Form drag is modeled using the following equation and applied in the opposite direction of the drift direction [25]:

$$F_{drag} = \frac{1}{2}\rho_w C_D A_w U_w^2 \tag{5}$$

where ρ_w is the density of sea-water, C_D is the drag coefficient and assumed to be a function of ship draft to length ratio (see [25] for details), A_w is submerged cross section area, and U_w is the forced drift velocity.

Since the forced drift speed and direction are initially unknown, an iterative solution must be applied. Therefore, the first estimate of drift speed and direction is based only on the wind and wave drift forces. This estimate of drift speed is taken and used to compute estimates of the form drag and wave damping. The full equations are then used to calculate a revised and final estimate of drift speed and direction. This is repeated until a stable solution is obtained.

3.2. Time to ground (TTG)

After obtaining the estimate of drift speed, v_d and direction, θ_0, we use the vessel coordinates (x, y) and surrounding water depth information to measure the distance until grounding. Drift speed is modeled as a constant value, and the direction is assumed to follow a normal distribution, centered on θ_0, and with a standard deviation, σ, of 20°. This value of standard deviation is based on previous experimental results [25].

Water depth information is taken from the Norwegian Map authority's electronic navigation charts (ENC) [29]. Water depth information is presented as complex polygons with latitude and longitude coordinates. Each polygon contains information on the minimum and maximum depths within the polygon. All polygons for which the minimum depth is less than one and a half times the operational draft of the ship are marked as potential grounding hazards.

For a given drift direction, we determine the minimum distance until grounding using the `shapely` package. The function determines the polygon intersections with the drift direction vector. The minimum of these distances is returned as the distance to ground for this angle and position, $s(x, y, \theta_0)$.

The TTG is then calculated as the expected value of drift direction divided by the drift speed. We integrate from 45° below to 45° above θ_0 of possible angles:

$$TTG(x, y) = \frac{\int_{\theta_0-\pi/4}^{\theta_0+\pi/4} s(x, y, \theta) \frac{1}{\sqrt{2\pi\sigma^2}} \exp\left(-\frac{(\theta-\theta_0)^2}{2\sigma^2}\right) d\theta}{|v_d(x, y)|} \tag{6}$$

The TTG is stored for each time stamp over the voyage.

3.3. Case study and data sources

To demonstrate the methodology, the research vessel (RV) *Gunnerus* is used, which is 36.25-m length overall (LOA) research vessel operated by NTNU. Physical ship characteristics for *Gunnerus* were determined from vessel drawings and plans. Vessel latitude and longitude positions were taken from the onboard voyage data

recorder (VDR).

Table 1 presents an overview of the variables and the data sources used to perform the analysis.

Table 1: Variable definitions and descriptions

Symbol	Description	Value	Units	Notes
Ship characteristics				
L	Length between perpendiculars	33.9	m	Ship drawings
B	Breadth (moulded)	9.60	m	-
T	Ship operational draft	2.50	m	-
A_{cwp}	Cross wind profile (CWP) area	160.0	m^2	-
Operational variables				
x	Longitude	–	-	VDR
y	Latitude	–	-	-
Environmental conditions				
V_{wind}	Wind speed	–	m/s	MyWaveWAM800m
α	Wind direction	–	°	-
H_S	Significant wave height	–	m	-
T_p	Wave mean period	–	s	-
ϕ	Wave direction	–	°	-
$\boldsymbol{v_{Ox}}$	Sea-water x-velocity	–	m/s	Norkyst
$\boldsymbol{v_{Oy}}$	Sea-water y-velocity	–	m/s	-

The methodology is applied to a voyage on November 3 - 4, 2022 beginning near Ålesund and finishing in Trondheim. The path of the overall voyage is shown in Figure 1a. Coordinates were extracted approximately every 30 minutes and used to obtain environmental data. These points are labeled chronologically.

Historical environmental data on wind, waves, and sea-water velocities is taken from two forecast data models developed by the Norwegian Meteorological Institute. Wind and wave data is taken from historical forecasts generated by MyWaveWAM800m, which has a coastal resolution of 800m and temporal spacing of one hour. Norkyst, a coastal forecasting tool, is used to obtain information on the sea-water velocities [30].

4. RESULTS

The voyage begins near Otrøya (Point 0). Points 5-8 are the crossing of Hustadvika, an exposed area to the weather with a large number of shallow shoals. It was in this location that the *Viking Sky* nearly ran aground in 2019 following a loss of propulsion [9]. Points 9-13 show the *Gunnerus* returning to internal waterways in order to reach Kristiansund. The following day, *Gunnerus* departed Kristiansund (Point 14) and navigated through the Trondheimsleia between the mainland and the Smøla (16-18) and Hitra islands (19-23) before reaching the mouth of the Trondheimsfjord (Point 28). *Gunnerus* then sailed to its home port in Trondheim (Point 33).

The Norwegian Maritime Authority distinguishes trade areas according to their protection against waves and wind from the open sea. These designations include completely sheltered waters (Type 1), protected waters (Type 2), and areas where the unsheltered stretches do not exceed either 5 (Type 3) or 25 (Type 4) nautical miles [31]. Points classified as completely sheltered are 3-4, 9-12 (Kvernesfjorden), and 14. Protected points are 13 and 20-32 (Trondheimsleia and Trondheimsfjord). Points with unsheltered stretches less than 5 nm include 0-2 and 15-19. Points considered to be unprotected, i.e., the open sea, are 5-8 (Hustadvika).

Figure 1b displays the encountered wind speeds and significant wave heights at each index. The highest wave heights were encountered in Hustadvika (Points 5-8), while the highest wind speeds occurred as the ship entered the Trondheimsfjord (Points 25-31).

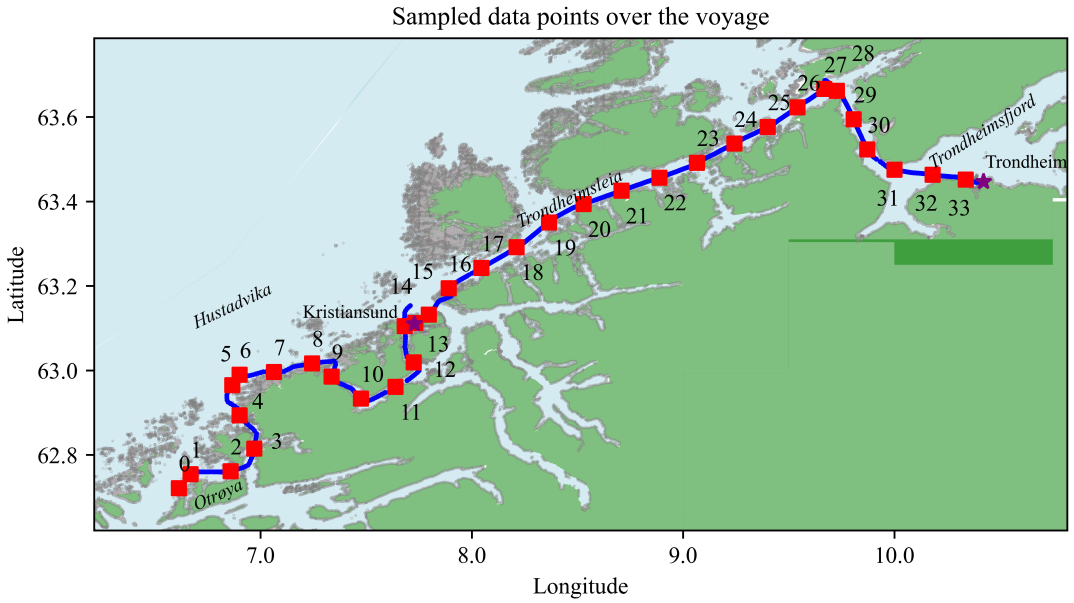

(a) Overall voyage from November 3-4, 2023. Sampled points are labeled.

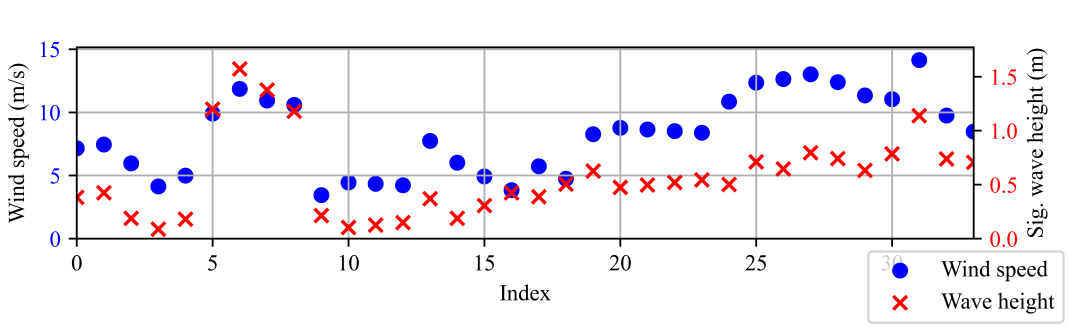

(b) Wind speed and wave heights from the sampled points during the voyage

Figure 1: Overall voyage plot and weather conditions.

Figures 2 and 3 present the coordinates with a vector indicating the predicted drift speed and direction for the given environmental conditions. On the left hand side, areas shaded in green represent land and areas shaded in pink represent grounding hazards including reefs and shoals. The right hand side displays the computed time until grounding for each coordinate. The dashed line marks one hour, the average repair time following a loss of propulsion according to previous research [19].

The first half of the voyage is shown in Figure 2. The predicted drift direction is consistently towards the south (0-9). The highest expected drift speeds are experienced from Points 5-8 while transiting the exposed section of the route. At point 7, the expected force drift speed is 0.57 m/s. Point 8 represents the minimum observed TTG (seven minutes) while transiting between two shoals. The expected TTG becomes much higher as the ship sails inland, reaching its observed maximum at point 10, due to a very low predicted drift speed.

Figure 3 presents the voyage from Kristiansund to Trondheim. Points 16-20 show an expected TTG between 1-2 hours. Very low drift speeds at Points 21-22 lead to much higher estimates of TTG before returning to values of 1-2 hours at points 23-24. As the ship enters the Trondheimsfjord (point 25), the predicted drift direction begins to fluctuate significantly.

For all sampled points in the voyage, the wave height and drift speed are plotted as a function of wind speed in Figure 4. Furthermore, wind direction is plotted against both wave direction and the predicted drift angle.

Significant wave height generally increases as wind speed increases, consistent with oceanographic principles.

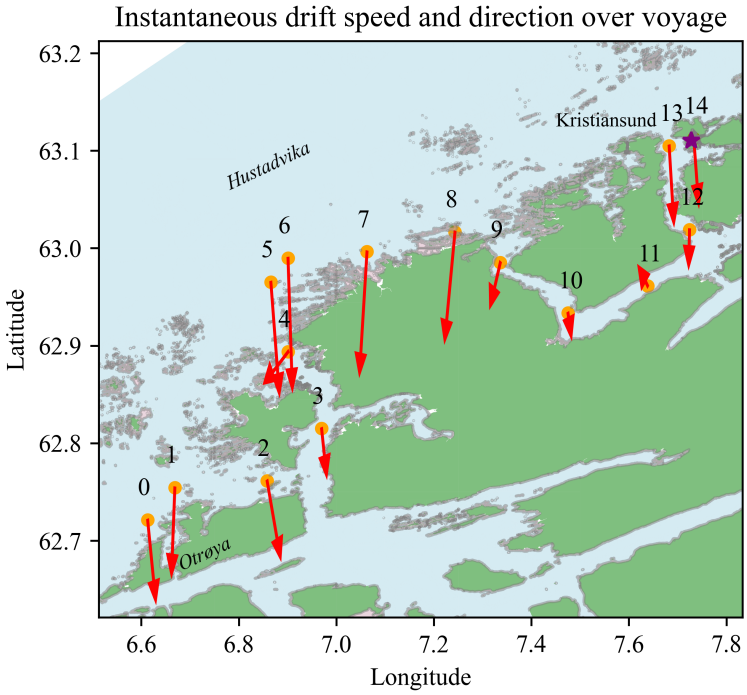

(a) Part 1: Otrøya to Kristiansund with drift projections. Arrow corresponds to overall predicted drift speed and direction (max value of 0.57 m/s occurs at Point 7).

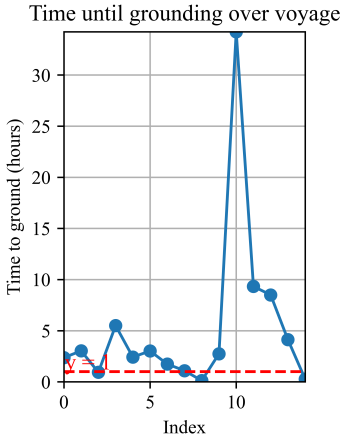

(b) TTG during the voyage

Figure 2: First half of the voyage

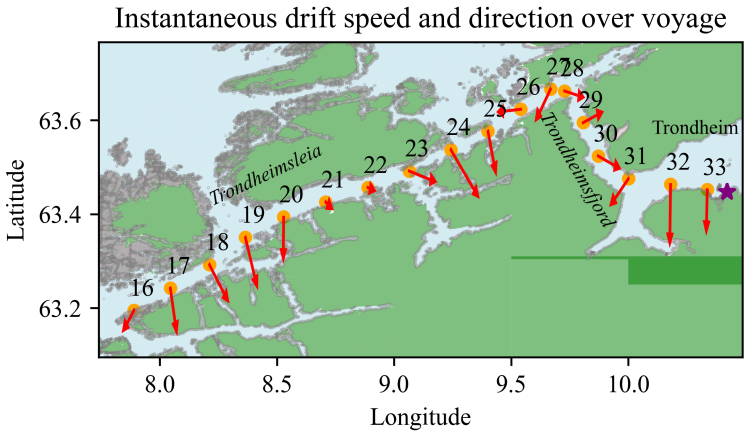

(a) Part 2: Kristiansund to Trondheim with drift projections. Arrow corresponds to overall predicted drift speed and direction (max value of 0.66 m/s occurs at Point 24).

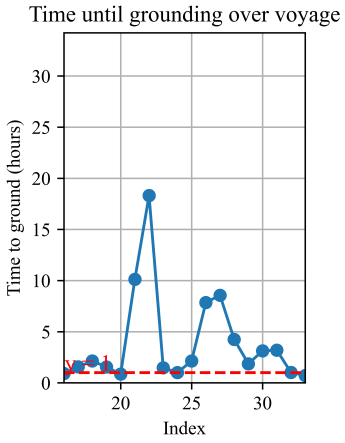

(b) TTG during the voyage

Figure 3: Second half of the voyage

Similarly, there is a positive relationship between wind speed and drift speed. There is moderate agreement between wind and wave direction, although wave direction is frequently out of phase with wind direction. This results in the scatter in the relationship between forced drift direction and wind direction.

5. DISCUSSION

5.1. Summary of findings

This study develops a risk indicator for the early warning of ship drifting groundings that incorporates the relevant information on the ship's location, environmental conditions, and surrounding grounding hazards. Ad-

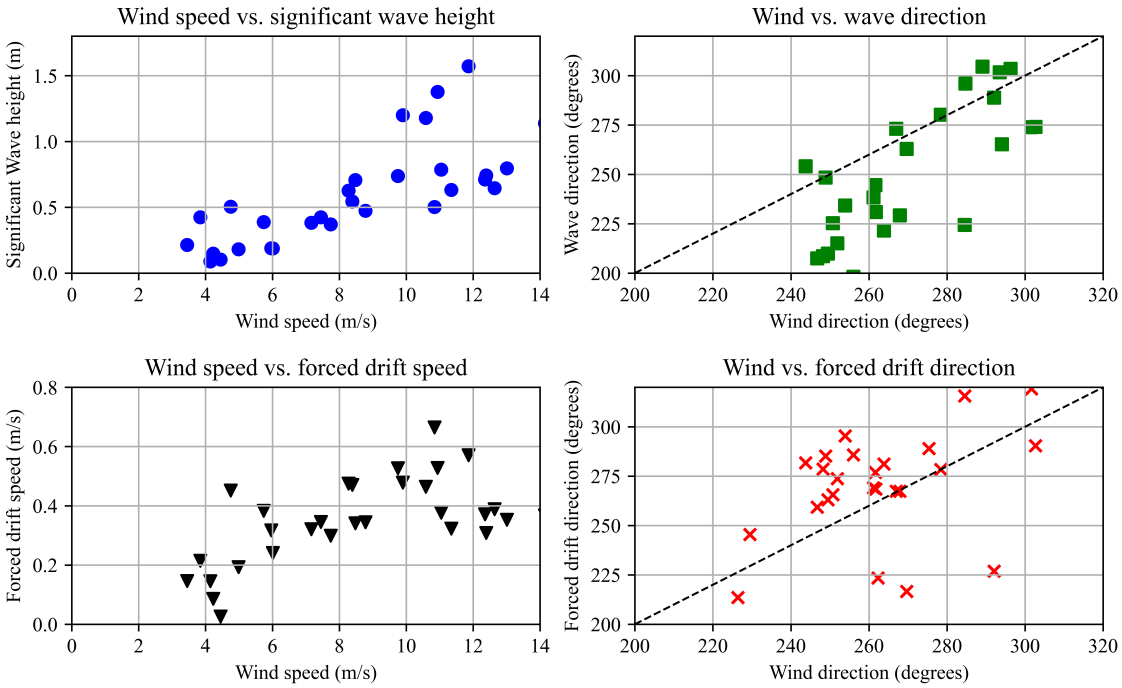

Figure 4: Observed relationships between encountered weather conditions and forced drift

ditionally we aim to identify how the TTG varies over a voyage with different navigational and environmental conditions. The case study shows that the TTG varies significantly over the course of a voyage, and can frequently drop below the average repair time of machinery failures, posing a critical risk if the ship were to suffer a loss of propulsion at these points.

The use of such an indicator in traffic monitoring systems allows for identification of high risk ships and subsequent prioritization for VTS operators [32] [33]. Furthermore, Berg et al. [11] shows how VTS responded to near misses in Norwegian waters after they occurred. Reevaluation of historical traffic data using a risk indicator allows for reconsidering the allocation of emergency response resources, including the placement and sizing of emergency tugboats [12].

Risk quantification is required for the expanded decision-making capabilities of autonomous system. Examples of control systems with anti-grounding functionality include [34] and [35]. However, these systems use the distance to shore to express grounding risk level. The use of TTG gives a better representation of the ship's actual condition; using the distance to ground does not incorporate the expected drift motion of the ship following a failure. The method proposed in this paper incorporates dynamic environmental conditions that update along with the ship's location and environmental conditions.

5.2. Limitations and future work

This work explores how the TTG varies over the duration of a typical voyage. For simplicity, only one drift prediction methodology has been used. Due to the assumptions previously mentioned, future work should compare different modeling approaches to evaluate two key issues. First is the behavior of ships by size and the resulting dominant forces (e.g., wind or waves). Sørgård and Vada [25] only examine ships between 250-270 meters overall. Wind damping was deemed negligible for ships of this size, but this should be confirmed when the methodology is applied to smaller ships. The predictions should be compared to observations of drifting ships wherever possible.

Furthermore, the probabilistic approach simplifies the actual drifting behavior of the ship. This approach assumes constant wind and weather values to predict drifting behavior. In reality, the wind and weather conditions will change both over time and by position. This simplification is mostly relevant for predicted TTGs greater

than a few hours.

TTG may play an important role during risk based voyage planning. For example, the TTG can be calculated for different voyage alternatives and for determining between alternative routes. The use of TTG can be combined with measures of machinery health to estimate the dynamic probability of failure. This problem may then be explored as a decision-making model for a risk based controller to influence decisions relating to the operation of the machinery system, e.g., switching between operational modes, as criteria for the start/stop of redundant propulsion equipment, or deciding to sail further from shore.

6. CONCLUSION

This paper demonstrates the methodology and data sources required to develop a risk indicator for the early warning of drifting groundings. TTG considers the ship's environmental conditions and grounding hazards to better present the risk associated with this accident mode. The TTG can potentially improve the monitoring of coastal traffic or be used within a risk based controller to improve onboard risk perception for autonomous systems.

Acknowledgments

This work was supported by the Research Council of Norway through the Centers for Research-Driven Innovation funding scheme, project number 309230 - SFI Autoship.

References

[1] G. Conan, G. M. Dunnet, D. J. Crisp, H. A. Cole, R. Clark, The long-term effects of the Amoco Cadiz oil spill, Philosophical Transactions of the Royal Society of London. B, Biological Sciences 297 (1983) 323–333. doi:10.1098/rstb.1982.0045, publisher: Royal Society.

[2] K. Tazaki, A. Fukuyama, F. Tazaki, Y. Shintaku, K. Nakamura, T. Takehara, Y. Katsura, K. Shimada, Twenty Years after the Nakhodka Oil Spill Accident in the Sea of Japan, How Has Contamination Changed?, Minerals 8 (2018) 178. doi:10.3390/min8050178, number: 5 Publisher: Multidisciplinary Digital Publishing Institute.

[3] NTSB, Fire Aboard the Tug Scandia and the Subsequent Grounding of the Tug and the Tank Barge North Cape on Moonstone Beach, South Kingston, Rhode Island, January 19, 1996, Technical Report MAR-98/03, NTSB, 1998.

[4] NTSB, Grounding of Malaysian-flag Bulk Carrier M/V Selendang Ayu on North Shore of Unalaska Island, Alaska, December 8, 2004, Technical Report DCA-05-MM-008, NTSB, 2005.

[5] IMO, Guidelines for Vessel Traffic Services, 2022.

[6] NTSB, Grounding of Bulk Carrier Nenita, Technical Report MAB-18/01, NTSB, 2018.

[7] MAIB, Report on the investigation of the grounding and recovery of the container feeder vessel Thea II and the tug Svitzer Josephine in the approaches to the Humber Estuary on 15 December 2018, Technical Report 15/2020, MAIB, 2018.

[8] BEA MER, Grounding of the bunker tanker TRESTA STAR on the 3rd of February 2022, nearby Pointe du Tremblet (La Réunion), Technical Report, BEA MER, 2023.

[9] Norwegian Safety Investigation Authority, Loss of propulsion and near grounding of Viking Sky, Hustadvika, Norway 23 March 2019, Technical Report Marine 2024/05, NSIA, 2024.

[10] Marine Safety Investigation Unit, Safety investigation into the loss of control of the Maltese registered bulk carrier JULIETTA D, Technical Report 02/2023, Transport Malta, 2023.

[11] T. Berg, O. Selvik, R. Indergaard, E. Ringen, Maritime Emergency Preparedness – Drifting Ships, IOP Conference Series: Materials Science and Engineering 1288 (2023) 012001. doi:10.1088/1757-899X/1288/1/012001, publisher: IOP Publishing.

[12] B. Assimizele, J. O. Royset, R. T. Bye, J. Oppen, Preventing environmental disasters from grounding accidents: A case study of tugboat positioning along the Norwegian coast, Journal of the Operational Research Society 69 (2018) 1773–1792. doi:10.1080/01605682.2017.1409157, publisher: Taylor & Francis _eprint: https://doi.org/10.1080/01605682.2017.1409157.

[13] M. Rausand, S. Haugen, Risk assessment: theory, methods, and applications, Wiley series in statistics in practice, John Wiley & Sons, Hoboken, NJ, 2020.
[14] K. Øien, I. Utne, I. Herrera, Building Safety indicators: Part 1 – Theoretical foundation, Safety Science 49 (2011) 148–161. doi:10.1016/j.ssci.2010.05.012.
[15] K. Øien, I. Utne, R. Tinmannsvik, S. Massaiu, Building Safety indicators: Part 2 – Application, practices and results, Safety Science 49 (2011) 162–171. doi:10.1016/j.ssci.2010.05.015.
[16] A. Mazaheri, J. Montewka, P. Kujala, Modeling the risk of ship grounding—a literature review from a risk management perspective, WMU Journal of Maritime Affairs 13 (2014) 269–297. doi:10.1007/s13437-013-0056-3.
[17] IMO, Revised harmonized reporting procedures - Reports required under SOLAS regulations I21, Technical Report MSC-MEPC.3-Circ.4 Rev 1, IMO, 2014.
[18] T. G. Fowler, E. Sørgård, Modeling Ship Transportation Risk, Risk Analysis 20 (2000) 225–244. doi:10.1111/0272-4332.202022.
[19] P. Friis-Hansen, Basic modelling principles for prediction of collision and grounding frequencies, 2007.
[20] Kystverket, Automated calculation of risk related to ship traffic, Technical Report, Kystverket, 2021.
[21] J. N. Newman, The drift forces and moment on ships in waves, David W. Taylor Model Basin, Washington DC, USA, Navy Department, Research and Development, From Advances in Applied Mechanics, Volume 18, pp. 221-283, Massachusetts (1965).
[22] M. Ueno, T. Nimura, On Steady Drifting Motion of a Ship in Waves, IFAC Proceedings Volumes 33 (2000) 387–392. doi:10.1016/S1474-6670(17)37105-7.
[23] H. Yasukawa, N. Hirata, Y. Nakayama, A. Matsuda, Drifting of a dead ship in wind, Ship Technology Research 70 (2023) 26–45. doi:10.1080/09377255.2021.1954835, publisher: Taylor & Francis _eprint: https://doi.org/10.1080/09377255.2021.1954835.
[24] H. Yasukawa, R. Okuda, M. A. A. Hasnan, Y. Nakayama, A. Matsuda, 6-DOF motion simulations of a deadship drifting in wind and waves, Ocean Engineering 275 (2023) 114158. doi:10.1016/j.oceaneng.2023.114158.
[25] E. Sørgård, T. Vada, Observations and modelling of drifting ships, Technical Report 96-2011, DNV, 1998.
[26] K.-F. Dagestad, J. Röhrs, O. Breivik, B. Ådlandsvik, OpenDrift v1.0: a generic framework for trajectory modelling, Geoscientific Model Development 11 (2018) 1405–1420. doi:10.5194/gmd-11-1405-2018, publisher: Copernicus GmbH.
[27] O. M. Mazzaretto, M. Menéndez, H. Lobeto, A global evaluation of the JONSWAP spectra suitability on coastal areas, Ocean Engineering 266 (2022) 112756. doi:10.1016/j.oceaneng.2022.112756.
[28] K. Hasselmann, T. P. Barnett, E. Bouws, H. Carlson, D. E. Cartwright, K. Enke, J. A. Ewing, H. Gienapp, D. E. Hasselmann, P. Kruseman, A. Meerburg, P. Müller, D. J. Olbers, K. Richter, W. Sell, H. Walden, Measurements of wind-wave growth and swell decay during the Joint North Sea Wave Project (JONSWAP), Ergänzungsheft 8-12 (1973). Publisher: Deutches Hydrographisches Institut.
[29] Kartverket, Elektroniske sjøkart (ENC), 2023.
[30] J. Albretsen, A. K. Sperrevik, A. Staalstrøm, A. D. Sandvik, F. Vikebø, L. Asplin, NorKyst-800 Report No. 1: User Manual and technical descriptions, Technical Report, Havforskningsinstituttet, 2011.
[31] Nærings- og fiskeridepartementet, Forskrift om fartsområder, 1982.
[32] M. S. Eide, O. Endresen, P. O. Brett, J. L. Ervik, K. Røang, Intelligent ship traffic monitoring for oil spill prevention: Risk based decision support building on AIS, Marine Pollution Bulletin 54 (2007) 145–148. doi:10.1016/j.marpolbul.2006.11.004.
[33] M. S. Eide, O. Endresen, O. Breivik, O. W. Brude, I. H. Ellingsen, K. Roeang, J. Hauge, P. O. Brett, Prevention of oil spill from shipping by modelling of dynamic risk, Marine Pollution Bulletin 54 (2007) 1619–1633. doi:10.1016/j.marpolbul.2007.06.013.
[34] T. Tengesdal, T. A. Johansen, T. D. Grande, S. Blindheim, Ship Collision Avoidance and Anti Grounding Using Parallelized Cost Evaluation in Probabilistic Scenario-Based Model Predictive Control, IEEE Access 10 (2022) 111650–111664. doi:10.1109/ACCESS.2022.3215654.
[35] S. Blindheim, B. Rokseth, T. A. Johansen, Autonomous Machinery Management for Supervisory Risk Control Using Particle Swarm Optimization, Journal of Marine Science and Engineering 11 (2023) 327. doi:10.3390/jmse11020327.